Thermalization of Light's Orbital Angular Momentum in Nonlinear Multimode Waveguide Systems

Fan O. Wu[1], Qi Zhong,[1] Huizhong Ren,[1] Pawel S. Jung,[1,2]
Konstantinos G. Makris[3,4] and Demetrios N. Christodoulides[1,*]

[1]*CREOL/College of Optics and Photonics, University of Central Florida, Orlando, Florida 32816, USA*
[2]*Faculty of Physics, Warsaw University of Technology, Koszykowa 75, 00-662 Warsaw, Poland*
[3]*ITCP-Department of Physics, University of Crete, P.O. Box 2208, 71003 Heraklion, Greece*
[4]*Institute of Electronic Structure and Laser, Foundation for Research and Technology-Hellas, P.O. Box 1527, 71110 Heraklion, Greece*

We show that the orbital angular momentum (OAM) of a light field can be thermalized in a nonlinear cylindrical multimode optical waveguide. We find that upon thermal equilibrium, the maximization of the optical entropy leads to a generalized Rayleigh-Jeans distribution that governs the power modal occupancies with respect to the discrete OAM charge numbers. This distribution is characterized by a temperature that is by nature different from that associated with the longitudinal electromagnetic momentum flow of the optical field. Counterintuitively and in contrast to previous results, we demonstrate that even under positive temperatures, the ground state of the fiber is not always the most populated in terms of power. Instead, because of OAM, the thermalization processes may favor higher-order modes. A new equation of state is derived along with an extended Euler equation resulting from the extensivity of the entropy itself. By monitoring the nonlinear interaction between two multimode optical wave fronts with opposite spins, we show that the exchange of angular momentum is dictated by the difference in OAM temperatures, in full accord with the second law of thermodynamics. The theoretical analysis presented here is corroborated by numerical simulations that take into account the complex nonlinear dynamics of hundreds of modes. Our results may pave the way toward high-power optical sources with controllable orbital angular momenta, and at a more fundamental level, they may open up opportunities in drawing parallels with other complex multimode nonlinear systems like rotating atomic clouds.

Angular momentum plays a pivotal role in physics. In settings with a continuous rotational symmetry, Noether's theorem [1,2] dictates that this quantity is conserved, an aspect that governs both the macroscopic and microscopic behaviors of a multitude of physical systems. These could range from the dynamics of spiral galaxies [3], pulsars [4], and neutron stars to the intriguing properties of quantum vortices in superfluids [5] and rotating atomic clouds [6–8]. The fact that the electromagnetic field carries spin and/or orbital angular momentum (OAM) was recognized early on with the advent of Maxwell's electrodynamics [9,10]. Yet, it is only recently that the angular momentum of light was recognized as a new degree of freedom through which a wealth of opportunities could open up within the discipline of optics and photonics [11–14]. In this respect, the orbital angular momentum of light has been systematically used in manipulating and guiding atoms [15], in optical vortex soliton interactions [16,17], in microscopies [18], optical ablation [19], quantum entanglement [20–22], astronomy [23–26], and high-speed communication systems [27,28], to mention a few. Similar ideas have lately permeated the area of statistical optics as well as the new emerging field of optical metasurfaces where new methodologies have

been developed to generate and detect OAM light states [29–33].

On the other hand, the way angular momentum appears in statistical mechanics is more subtle. As indicated by Jaynes [34] and Callen [35], if the OAM $\vec{L}$ is a constant of the motion, it can then assume the role of an extensive variable in addition to that of the energy. As such, it must be paired with an intensive quantity or a generalized force that acts as a "temperature" in the canonical distribution function. Under these conditions, one should expect that the entropy of the system must also be extensive with respect to the OAM, thus satisfying a key postulate of thermodynamics. Interestingly, OAM thermalization effects have been considered in the past in connection with rotating atomic gases [6–8] when studied in the canonical ensemble. In such rotating canonical settings, a modified energy landscape can be introduced [36] by means of which the rotational speed Ω can be interpreted as the conjugate temperature corresponding to the OAM. As we will see, the situation in nonlinear optical environments is different. While there are similarities with the case of rotating bosonic gases, in optics, the notion of relying on an underlying rotational speed Ω is absent. At a more
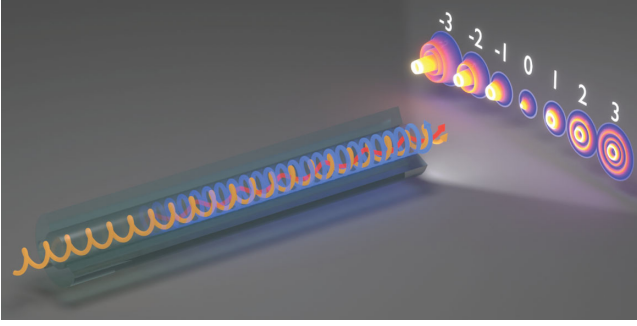
FIG. 1. The OAM of light propagating in a multimode cylindrical structure can be thermalized because of nonlinearity in a way that favors either positive or negative OAM numbers.

fundamental level, what sets these two physical systems apart is the fact that a nonlinear multimode photonic system behaves as a microcanonical ensemble after reaching thermal equilibrium in isolation.

In this Letter, we show for the first time, that the OAM of a light beam propagating in a nonlinear cylindrical waveguide structure can be irreversibly thermalized in a manner that directly depends on the discrete OAM number of a particular mode. Even more importantly, upon attaining thermal equilibrium, the OAM is now governed by its own optical temperature T_L—a temperature that is the thermodynamic conjugate of the OAM in this microcanonical optical system (Fig. 1). In this respect, a generalized Rayleigh-Jeans distribution can be derived, that even under positive temperature (T_U) conditions, does not always favor the ground state. New equations of state are obtained that relate the extensive variables with their corresponding generalized forces. Finally, based on entropic principles, we show that the OAM temperature T_L is a true thermodynamic quantity in the sense that it dictates the OAM exchange between two optical beams of opposite spin when traversing a nonlinear medium. The predicted theoretical results are in excellent agreement with numerical simulations.

To this end, let us consider a weakly guiding, nonlinear cylindrical waveguide having a normalized refractive index distribution $V(r)$, where r represents the cylindrical radial coordinate. In Kerr nonlinear media, the optical field $u(x, y, z)$ evolution along the z direction is governed by the normalized nonlinear Schrödinger equation:

$$i\frac{\partial u}{\partial z} + \left(\frac{\partial^2 u}{\partial x^2} + \frac{\partial^2 u}{\partial y^2}\right) + V(x, y)u + |u|^2 u = 0. \quad (1)$$

In this system, the field orbital angular momentum is given by $\vec{L} = \iint_{-\infty}^{\infty} \vec{r} \times \vec{p}\,dxdy$, where $\vec{p} = (i/2)(u\nabla_\perp u^* - u^*\nabla_\perp u)$ is the transverse momentum density, and $\nabla_\perp = \hat{x}(\partial/\partial x) + \hat{y}(\partial/\partial y)$. Given that $\vec{L}\|\hat{z}$, from this point on, L will be treated as a scalar quantity. The conservation laws C

associated with Eq. (1) are known to satisfy $\{C, H\}_{u,\pi} = \iint_{-\infty}^{\infty}[(\delta C/\delta u)(\delta H/\delta \pi) - (\delta H/\delta u)(\delta C/\delta \pi)]dxdy = 0$, where $\mathcal{H} = -i(u_x\pi_x + u_y\pi_y) + iVu\pi + \frac{1}{2}u^2\pi^2$ is the system's Hamiltonian density, $\pi = iu^*$ is the canonical field momentum, $\{\cdot\}$ denotes a Poisson bracket, and δ represent functional derivatives. In addition to the total power $\mathcal{P} = \iint_{-\infty}^{\infty}|u|^2 dxdy$ that remains constant throughout propagation, one can show that in a fully cylindrical structure $[V(x, y) = V(r)]$, the field orbital angular momentum L is also an invariant in this nonlinear system (see Supplemental Material [37]).

In general, an optical field propagating in the aforementioned cylindrical waveguide (supporting M modes) can be represented as a superposition of its underlying bound states $\psi_n(r, \phi, z) = R_n(r)e^{i\varepsilon_n z}e^{il_n\phi}$, i.e., $u = \sum_{n=1}^M c_n\psi_n$. Here, ε_n stands for the propagation constant or eigenvalue of the eigenmode ψ_n, $l_n \in \{0, \pm 1, \pm 2, \ldots\}$ denotes its discrete OAM charge, $R_n(r)$ is the radial part of the eigenfunction, while the complex number $c_n(z)$ describes the power occupancy ($|c_n|^2$) of this state during propagation. In this representation, the power and OAM invariants can be written as $\mathcal{P} = \sum_{n=1}^M |c_n|^2$ and $L = \sum_{n=1}^M l_n|c_n|^2$ [37]. On the other hand, the Hamiltonian constant of the motion $H = \iint_{-\infty}^{\infty}\mathcal{H}dxdy$ involves both a linear ($-U$) and a nonlinear component (H_{NL}), that is, $H = -U + H_{\text{NL}}$. Given that the system is operating in the weakly nonlinear regime, one finds that the Hamiltonian is dominated by its linear contribution, and as a result the quantity $U = -\sum_{n=1}^M \varepsilon_n|c_n|^2$ now assumes the role of the third invariant [38–42]. Interestingly, this "internal optical energy" U is associated with the Minkowski longitudinal electromagnetic momentum flowing in this guiding arrangement [43].

The existence of these three invariants $(\mathcal{P}, U, L)$ in this weakly nonlinear heavily multimode optical fiber now allows one to deploy principles from statistical mechanics. What facilitates this approach is the absence of required conservation laws $(M - 3)$, an aspect that leads to chaotic or wave turbulent behavior [38,44] in the evolution of the modal occupancies $|c_n(z)|^2$ and therefore allows the system to ergodically explore its phase space. In other words, all possible microstates $(c_1, \ldots, c_M)$ that lie on the manifolds of constant angular momentum (L), power ($\mathcal{P}$), and energy (U) are accessed with equal probability because of nonlinearity. To derive the state functions that relate the thermodynamically extensive variables $(\mathcal{P}, U, L, M)$ to the entropy S, we adopt a grand canonical description in a phase space constructed by $J_n \equiv |c_n|^2$ ($n = 1, 2, \ldots, M$) [45]. In this grand canonical frame, the local state of the system is described by a normalized probability density distribution $\rho(J_1, \ldots, J_M)$ where $\int_0^\infty \rho(J_1, \ldots, J_M) \times \prod_{n=1}^M dJ_n = 1$. Once the system attains thermal equilibrium, the average values of $\mathcal{P}$, L, and U serve as the invariants of this grand canonical system. In turn, the

probability density ρ can be used to construct the Gibbs entropy

$$S = -\int_0^\infty \rho(J_1, \ldots, J_M) \ln \rho(J_1, \ldots, J_M) \prod_{n=1}^M dJ_n, \quad (2)$$

which can be maximized by means of Lagrange multipliers, i.e.,

$$\rho(J_1, \ldots, J_M) = \frac{e^{\alpha \mathcal{P}(J_1, \ldots, J_M) + \beta U(J_1, \ldots, J_M) + \gamma L(J_1, \ldots, J_M)}}{\mathcal{Z}}, \quad (3)$$

where α, β, and γ represent constants associated with the three invariants. In this case, the generalized grand partition function is given by [37]

$$\mathcal{Z} = \int_0^\infty e^{\alpha \sum_{n=1}^M J_n - \beta \sum_{n=1}^M \varepsilon_n J_n + \gamma \sum_{n=1}^M l_n J_n} \prod_{n=1}^M dJ_n \quad (4a)$$

$$= \prod_{n=1}^M \frac{1}{-\alpha + \beta \varepsilon_n - \gamma l_n}. \quad (4b)$$

At equilibrium, the mean value $\langle J_m \rangle = \langle |c_m|^2 \rangle = \int_0^\infty \rho(J_1, \ldots, J_M) J_m \prod_{n=1}^M dJ_n$ can be directly obtained from the generalized partition function $\mathcal{Z}$ through the relations $\langle J_m \rangle = (1/\beta)(\partial \ln \mathcal{Z}/\partial \varepsilon_m) = -(1/\gamma)(\partial \ln \mathcal{Z}/\partial l_m)$ [37]. From here, one can find that $\langle J_m \rangle = [(-1)/(\alpha - \beta \varepsilon_m + \gamma l_m)]$. We then introduce two intensive quantities by defining $\beta \equiv -1/T_U$ and $\gamma \equiv -1/T_L$, i.e., an energy temperature T_U and an OAM temperature T_L that are conjugate to the extensive variables U and L, respectively. Here, α is another intensive quantity that is conjugate to $\mathcal{P}$, which serves as the chemical potential of the system. As a result, upon thermalization, the average power occupancy of each mode is found to obey a generalized Rayleigh-Jeans distribution

$$\langle |c_n|^2 \rangle = \frac{-1}{\alpha + \frac{\varepsilon_n}{T_U} - \frac{l_n}{T_L}}. \quad (5)$$

The generalized Rayleigh-Jeans distribution in Eq. (5) resulting from a generalized Gibbs ensemble [46,47] is central in this work. It implies that not only the internal energy U can be thermalized (via eigenvalue ε_n), but also the OAM since it explicitly involves the topological charge of the mode l_n—an aspect that has a profound effect on the modal power distributions (Fig. 1). Because of OAM, the possibility exists that the ground state (the lowest-order mode) is no longer the most populated in terms of power. Even more importantly, T_L is a true thermodynamic quantity that governs the flow of OAM between two optical beams. Note that, in our formalism, the "hot" and "cold" relative temperature axes are assigned with respect to the angular momenta, which in our designation is positive for right-handed OAM or negative for left-handed

OAM. This consistently ensures that angular momentum always flows from a hot subsystem to a cold subsystem in full agreement with the second law of thermodynamics. From this generalized distribution, the following global equation of state can be derived [37]:

$$-\alpha \mathcal{P} + \frac{U}{T_U} + \frac{L}{T_L} = M, \quad (6)$$

which relates the three intensive variables α, T_U, and T_L to the four extensive quantities $\mathcal{P}$, U, L, and M. We note that the inclusion of the number of modes M in the equation of state (6) is of paramount importance since it not only removes the "ultraviolet" divergence (for a finite number of modes) but also guarantees the very extensivity of our thermodynamic formalism.

Based on these premises, one can formally show that the entropy S of this optical multimode system can be directly expressed in terms of the modal occupancies via $S = \sum_{n=1}^M \ln(\langle |c_n|^2 \rangle)$ [37,38,43,45,48]. In addition, the fundamental equation of thermodynamics demands that $S = S(\mathcal{P}, U, L, M)$. Hence, two temperatures can be entropically defined through $T_U^{-1} \equiv \partial S/\partial U$ and $T_L^{-1} \equiv \partial S/\partial L$. Similarly, a generalized chemical potential α and an optical thermodynamic pressure $\tilde{p}$ can also be introduced using $\alpha \equiv -\partial S/\partial \mathcal{P}$ and $\tilde{p} \equiv \partial S/\partial M$ [37]. From here, a corresponding Euler equation can be obtained, which is a direct manifestation of the extensivity of the entropy itself with respect to $(\mathcal{P}, U, L, M)$,

$$S = -\alpha \mathcal{P} + \frac{U}{T_U} + \frac{L}{T_L} + \tilde{p}M. \quad (7)$$

In what follows, we corroborate our theoretical formalism by performing a series of numerical simulations in nonlinear parabolic and step-index optical fibers. In this respect, the results presented in Eqs. (5) and (6) will be employed to predict the OAM thermalization once equilibrium conditions are attained. As a first example, let us consider a parabolic silica fiber having $M = 120$ modes, conveying in total 100 kW of power at a wavelength of 1064 nm [37]. For this case, 62 modes of this fiber are evenly excited [Fig. 2(a)]. In normalized units, these launching conditions correspond to $\mathcal{P} = 100$, $U = -1468$, and $L = -140$. For this scenario, our theory predicts that at thermal equilibrium, the propagating optical wave front is expected to settle into an OAM temperature $T_L = 14.5$, an energy temperature $T_U = 15.2$, and a generalized chemical potential $\alpha = -2.26$. To verify these predictions, we numerically solved Eq. (1) under the same initial conditions. For each run, we allowed the phases of the input c_n coefficients to statistically vary in order to construct the statistical ensembles. Figures 2(b) and 2(c) show that an excellent agreement exists between the theoretically anticipated results and the numerical computations after OAM thermal equilibrium is reached at ~ 1 m of propagation. In this case, the modal
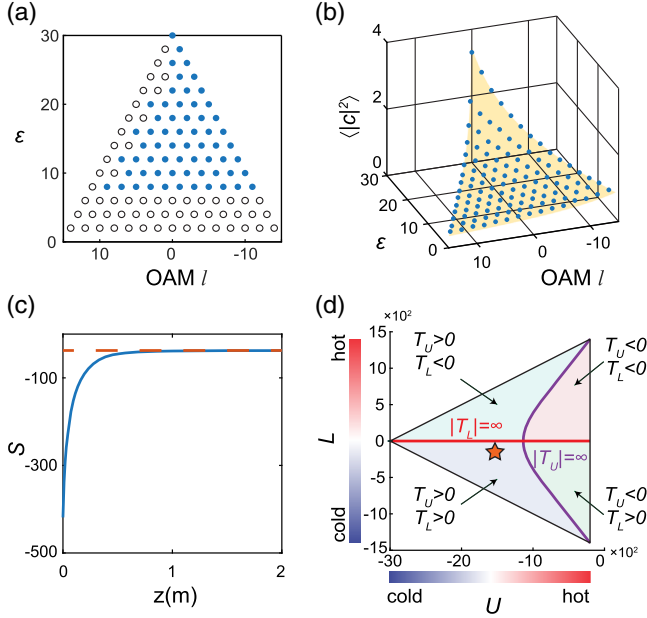
FIG. 2. Thermalization dynamics of the OAM associated with an optical beam propagating in a nonlinear parabolic graded-index fiber. (a) Initially, equally excited modes (blue dots) are plotted on the $\varepsilon - l$ triangular eigenvalue grid of a parabolic fiber. (b) The theoretically predicted modal occupancies $\langle|c_n|^2\rangle$ (yellow surface) are in excellent agreement with those obtained from numerical simulations (blue dots). The fluctuations associated with the modal occupancies are described in Ref. [37]. (c) During propagation, the optical entropy monotonically increases (blue curve) until it reaches its maximum value predicted from Eq. (5). (d) Depending on initial conditions (U, L), the system can settle into four different temperature regimes which are separated by the infinite temperature curves of energy (red) and OAM (purple). The red star denotes the initial (U, L) quantities that lead to (b) with $T_U > 0$, $T_L > 0$.

occupancies $\langle|c_n|^2\rangle$ are displayed on a two-dimensional triangular map that is specified by the accessible normalized propagation constants ε_n and OAM numbers l_n associated with the optical modes. For these initial conditions, the energy temperature T_U is positive, and therefore, the fundamental mode (LP$_{01}$) is the one mostly populated. Meanwhile, the OAM temperature T_L so happens to be positive, in which case, the optical power resides mostly in the left-handed rotating modes with negative OAM charges ($l_n < 0$). It is important to note that, in all cases, the initial conditions uniquely determine the equilibrium intensive variables (T_L, T_U, α) of this system. As Fig. 2(d) shows, both positive and negative T_L temperatures are possible, favoring left-handed and right-handed OAM groups of modes, respectively. Given that the OAM numbers in a cylindrical structure always come in pairs ($\pm l$), if the input OAM is zero, the system will relax into an infinite T_L temperature [Fig. 2(d)], which leads to OAM equipartition, and hence, the Rayleigh-Jeans distribution of Eq. (5) assumes a standard form [44].
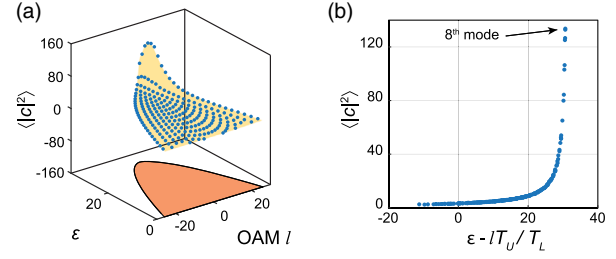

FIG. 3. Thermalization OAM dynamics associated with an optical beam propagating in a nonlinear step-index optical fiber. (a) The theoretically predicted modal occupancies $\langle|c_n|^2\rangle$ lying on the yellow surface are in good agreement with those obtained from numerical simulations (blue dots). For this example, the OAM temperature is negative, while the energy temperature is positive. Note that the $\varepsilon - l$ diagram (orange area) of a step-index fiber has now a paraboliclike shape. (b) Modal occupancies as a function of $(\varepsilon - lT_U/T_L)$. For this particular example, $T_U/T_L = -0.5$, and as a result, instead of the ground state, the higher-order LP$_{+3,1}$ mode now conveys most of the power.

Our theory is universal in the sense that it can be deployed to predict OAM thermalization in any cylindrical multimode nonlinear structure. Figure 3(a) shows the results of OAM thermalization in a step-index fiber having $M = 234$ modes. For the step-index case, the $\varepsilon - l$ map now assumes a paraboliclike shape. For the excitation conditions used in this simulation, $\mathcal{P} = 3200$, $U = -75420$, and $L = 8776$, for which values our theory predicts $T_U = 104$, $T_L = -204$, and $\alpha = -0.04$. As Figs. 3(a) and 3(b) show, there is excellent agreement between the numerical simulations and the theoretically anticipated results. Counterintuitively, in this case, while the energy temperature T_U is positive, the fundamental mode (LP$_{01}$) is no longer the most populated. Instead, the eighth mode LP$_{+3,1}$ ($l = +3$) carries most of the power. This anomaly in the distribution results from the interplay between the more convolved $\varepsilon - l$ map that corresponds to a step-index fiber and the nonseparability of U and L in the generalized Rayleigh-Jeans distribution. To intuitively understand this behavior, one can assign effective eigenenergies in this map according to $\varepsilon_{n,\text{eff}} = \varepsilon_n - l_n T_U/T_L$ that angularly $[\theta = \arctan(T_U/T_L)]$ project these data into a standard Rayleigh-Jeans curve. This is illustrated in Fig. 3(b) where the eighth mode is the first in line to assume the role of an "effective ground state." In this respect, the ratio of the two temperatures T_U/T_L can be used to select the highest populated mode in this system [49,50].

Next, we show that the OAM temperature T_L is an actual thermodynamic force that governs the direction of OAM exchange between two subsystems, just like its energy counterpart. Figure 4(a) illustrates a scenario where two circularly polarized beams are launched in the same nonlinear parabolic silica fiber. In this case, the total electric field with components $|R\rangle$ and $|L\rangle$ can be written in terms
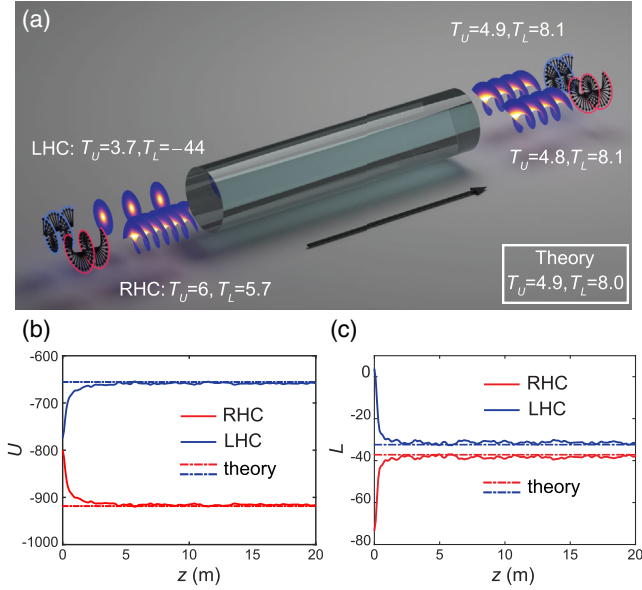
FIG. 4. (a) When a RHC beam conveying a significant negative OAM (red) and a LHC beam having almost zero OAM (blue) are launched into the same fiber, they eventually settle into the same energy temperature $T_U \approx 4.9$ and OAM temperature $T_L \approx 8.0$. During propagation, the longitudinal momentum U is transferred from the RHC to the LHC polarization (b), whereas the OAM flows in the opposite direction (c) given that initially $T_{U,u} > T_{U,v} > 0$ and $T_{L,v} < 0 < T_{L,u}$ (negative temperatures are hotter than positive).

of slowly varying envelopes (u, v) as $\vec{E} = u|R\rangle + v|L\rangle$, whose evolution equations can be found in Ref. [37]. In this arrangement, one can formally identify the following conservation laws [37]: $\mathcal{P}_u = \text{const}$, $\mathcal{P}_v = \text{const}$, $L_{\text{total}} = L_u + L_v = \text{const}$, and $U_{\text{total}} = U_u + U_v = \text{const}$. In the example that follows, the right-hand circularly (RHC) polarized light (red) is hotter in energy temperature T_U, while the left-handed circularly (LHC, blue) polarized light is hotter in terms of its OAM. Moreover, at the input $L_u(0) = -74$, $L_v(0) = 4 (L_{\text{total}} = -70)$, $\mathcal{P}_u = 50$, $\mathcal{P}_v = 40$, $U_u(0) = -800$, and $U_v(0) = -774 (U_{\text{total}} = -1574)$. While the two circular polarizations do not exchange power $\mathcal{P}$, they can exchange energy U and OAM L according to the second law of thermodynamics

$$dS_T = \left(\frac{1}{T_{U,u}} - \frac{1}{T_{U,v}} \right) dU_u + \left(\frac{1}{T_{L,u}} - \frac{1}{T_{L,v}} \right) dL_u \geq 0, \quad (8)$$

given that $dU_u = -dU_v$ and $dL_u = -dL_v$. As a result, during copropagation, both energy and OAM are exchanged until the two polarizations settle into the same temperatures $(T_{U,u} = T_{U,v}, T_{L,u} = T_{L,v})$, as expected from actual thermodynamic forces. Figures 4(b) and 4(c) demonstrate this behavior. Note that the equilibrium temperatures and chemical potentials can be directly predicted from the theoretical formalism [37].

In conclusion, we have shown that the OAM of a light beam propagating in a nonlinear cylindrical waveguide structure can be thermalized. A generalized Rayleigh-Jeans distribution has been derived that explicitly depends on the OAM charge. The interplay between energy and OAM can lead to an anomaly in the power distributions among modes, thus allowing higher-order modes to be favored. The exchange of OAM between two subsystems formally indicates that the OAM temperature acts like a true thermodynamic force. Before closing, we note that of interest would be to investigate whether some of the ideas presented above can be pursued in rotating atomic clouds where, for example, a two-component atomic gas (with each component having an opposite OAM) can be thermalized in a cylindrically symmetric trap. In addition, can anomalies in thermalization be observed in steplike anharmonic traps? The prospect of using similar notions in other fields of physics could be another interesting direction. It recently came to our attention that OAM thermalization has been experimentally observed in Ref. [51].

F. O. W. and Q. Z. contributed equally to this work.

---

[*] demetri@creol.ucf.edu

[1] W. J. Thompson, *Angular Momentum: An Illustrated Guide to Rotational Symmetries for Physical Systems* (Wiley, New York, 1994).

[2] C. Cîrstoiu, K. Korzekwa, and D. Jennings, Phys. Rev. X **10**, 041035 (2020).

[3] S. Genel, S. M. Fall, L. Hernquist, M. Vogelsberger, G. F. Snyder, V. Rodriguez-Gomez, D. Sijacki, and V. Springel, Astrophys. J. **804**, L40 (2015).

[4] H. O. de Oliveira and N. S. Magalhaes, Astron. Nachr. **342**, 255 (2021).

[5] T. Boulier, E. Cancellieri, N. D. Sangouard, Q. Glorieux, A. V. Kavokin, D. M. Whittaker, E. Giacobino, and A. Bramati, Phys. Rev. Lett. **116**, 116402 (2016).

[6] A. L. Fetter, Rev. Mod. Phys. **81**, 647 (2009).

[7] D. A. Butts and D. S. Rokhsar, Nature (London) **397**, 327 (1999).

[8] T. M. Wright, R. J. Ballagh, A. S. Bradley, P. B. Blakie, and C. W. Gardiner, Phys. Rev. A **78**, 063601 (2008).

[9] R. A. Beth, Phys. Rev. **50**, 115 (1936).

[10] J. D. Jackson, *Classical Electrodynamics*, 3rd ed. (Wiley, New York, 1998).

[11] A. M. Yao and M. J. Padgett, Adv. Opt. Photonics **3**, 161 (2011).

[12] Y. Shen, X. Wang, Z. Xie, C. Min, X. Fu, Q. Liu, M. Gong, and X. Yuan, Light Sci. Appl. **8**, 90 (2019).

[13] G. Molina-Terriza, J. P. Torres, and L. Torner, Nat. Phys. **3**, 305 (2007).

[14] A. Ramos, L. Fernández-Alcázar, T. Kottos, and B. Shapiro, Phys. Rev. X **10**, 031024 (2020).

[15] H. He, M. E. J. Friese, N. R. Heckenberg, and H. Rubinsztein-Dunlop, Phys. Rev. Lett. **75**, 826 (1995).

[16] G. A. Swartzlander and C. T. Law, Phys. Rev. Lett. **69**, 2503 (1992).

[17] Y. S. Kivshar and B. Luther-Davies, Phys. Rep. **298**, 81 (1998).

[18] X. Xie, Y. Chen, K. Yang, and J. Zhou, Phys. Rev. Lett. **113**, 263901 (2014).

[19] K. Toyoda, F. Takahashi, S. Takizawa, Y. Tokizane, K. Miyamoto, R. Morita, and T. Omatsu, Phys. Rev. Lett. **110**, 143603 (2013).

[20] A. Sit, F. Bouchard, R. Fickler, J. Gagnon-Bischoff, H. Larocque, K. Heshami, D. Elser, C. Peuntinger, K. Günthner, B. Heim, C. Marquardt, G. Leuchs, R. W. Boyd, and E. Karimi, Optica **4**, 1006 (2017).

[21] T. Stav, A. Faerman, E. Maguid, D. Oren, V. Kleiner, E. Hasman, and M. Segev, Science **361**, 1101 (2018).

[22] M. Erhard, R. Fickler, M. Krenn, and A. Zeilinger, Light Sci. Appl. **7**, 17146 (2018).

[23] M. Harwit, Astrophys. J. **597**, 1266 (2003).

[24] J. H. Lee, G. Foo, E. G. Johnson, and G. A. Swartzlander, Phys. Rev. Lett. **97**, 053901 (2006).

[25] G. A. Swartzlander, E. L. Ford, R. S. Abdul-Malik, L. M. Close, M. A. Peters, D. M. Palacios, and D. W. Wilson, Opt. Express **16**, 10200 (2008).

[26] F. Tamburini, B. Thidé, G. Molina-Terriza, and G. Anzolin, Nat. Phys. **7**, 195 (2011).

[27] G. Gibson, J. Courtial, M. J. Padgett, M. Vasnetsov, V. Pas'ko, S. M. Barnett, and S. Franke-Arnold, Opt. Express **12**, 5448 (2004).

[28] J. Wang, J.-Y. Yang, I. M. Fazal, N. Ahmed, Y. Yan, H. Huang, Y. Ren, Y. Yue, S. Dolinar, M. Tur, and A. E. Willner, Nat. Photonics **6**, 488 (2012).

[29] A. V. Kildishev, A. Boltasseva, and V. M. Shalaev, Science **339**, 1232009 (2013).

[30] D. L. Sounas, C. Caloz, and A. Alù, Nat. Commun. **4**, 2407 (2013).

[31] E. Karimi, S. A. Schulz, I. De Leon, H. Qassim, J. Upham, and R. W. Boyd, Light Sci. Appl. **3**, e167 (2014).

[32] E. Maguid, I. Yulevich, D. Veksler, V. Kleiner, M. L. Brongersma, and E. Hasman, Science **352**, 1202 (2016).

[33] R. C. Devlin, A. Ambrosio, N. A. Rubin, J. P. B. Mueller, and F. Capasso, Science **358**, 896 (2017).

[34] E. T. Jaynes, Phys. Rev. **106**, 620 (1957).

[35] H. B. Callen, *Thermodynamics and an Introduction to Thermostatistics*, 2nd ed. (Wiley, New York, 1985).

[36] L. D. Landau and E. M. Lifshitz, *Statistical Physics*, 3rd ed. (Elsevier, New York, 1980).

[37] See Supplemental Material at http://link.aps.org/supplemental/10.1103/PhysRevLett.128.123901 for the details of the proof of conservation laws of H, $\mathcal{P}$ and L, OAM in the bases of bound (mode) states, generalized grand partition function $\mathcal{Z}$, derivation of the first equation of state, two equivalent definitions of entropy, action variables and the complete phase space, intensive thermodynamic quantities, conservation of total energy and OAM for two circularly polarized beams, theoretical prediction of the final temperatures, additional simulation information, thermal fluctuation, and internal energy U and nonlinear Hamiltonian H_{NL}.

[38] F. O. Wu, A. U. Hassan, and D. N. Christodoulides, Nat. Photonics **13**, 776 (2019).

[39] H. Pourbeyram, P. Sidorenko, F. Wu, N. Bender, L. Wright, D. Christodoulides, and F. Wise, arXiv:2012.12110.

[40] E. V. Podivilov, D. S. Kharenko, V. A. Gonta, K. Krupa, O. S. Sidelnikov, S. Turitsyn, M. P. Fedoruk, S. A. Babin, and S. Wabnitz, Phys. Rev. Lett. **122**, 103902 (2019).

[41] P. Aschieri, J. Garnier, C. Michel, V. Doya, and A. Picozzi, Phys. Rev. A **83**, 033838 (2011).

[42] A. Picozzi, J. Garnier, T. Hansson, P. Suret, S. Randoux, G. Millot, and D. Christodoulides, Phys. Rep. **542**, 1 (2014).

[43] H. A. Haus and H. Kogelnik, J. Opt. Soc. Am. **66**, 320 (1976).

[44] S. Dyachenko, A. Newell, A. Pushkarev, and V. Zakharov, Physica (Amsterdam) **57D**, 96 (1992).

[45] K. G. Makris, F. O. Wu, P. S. Jung, and D. N. Christodoulides, Opt. Lett. **45**, 1651 (2020).

[46] T. Langen, S. Erne, R. Geiger, B. Rauer, T. Schweigler, M. Kuhnert, W. Rohringer, I. E. Mazets, T. Gasenzer, and J. Schmiedmayer, Science **348**, 207 (2015).

[47] A. C. Cassidy, C. W. Clark, and M. Rigol, Phys. Rev. Lett. **106**, 140405 (2011).

[48] N. K. Efremidis and D. N. Christodoulides, Phys. Rev. A **103**, 043517 (2021).

[49] V. Bretin, S. Stock, Y. Seurin, and J. Dalibard, Phys. Rev. Lett. **92**, 050403 (2004).

[50] B. Mukherjee, A. Shaffer, P. B. Patel, Z. Yan, C. C. Wilson, V. Crépel, R. J. Fletcher, and M. Zwierlein, Nature (London) **601**, 58 (2022).

[51] E. V. Podivilov, F. Mangini, O. S. Sidelnikov, M. Ferraro, M. Gervaziev, D. S. Kharenko, M. Zitelli, M. P. Fedoruk, S. A. Babin, and S. Wabnitz, arXiv:2112.13696.